Electric Power Systems Research 163 (2018) 329–337

Contents lists available at ScienceDirect

Electric Power Systems Research

journal homepage: www.elsevier.com/locate/epsr

On the statistical characterization of hybrid PLC-wireless channels

Thiago R. Oliveira[a,*], Antonio A.M. Picorone[b], Camila B. Zeller[c], Sergio L. Netto[d], Moises V. Ribeiro[e]

[a] Electronics Department, Federal Institute of Education, Science and Technology of the Southeast of Minas Gerais (IF Sudeste MG), Campus Juiz de Fora, Brazil
[b] Electrical Engineering Department, Federal University of Juiz de Fora (UFJF), Juiz de Fora, Brazil
[c] Statistical Department, Federal University of Juiz de Fora (UFJF), Juiz de Fora, Brazil
[d] Electrical Engineering Program at COPPE-Federal University of Rio de Janeiro (UFRJ), Rio de Janeiro, Brazil
[e] Electrical Engineering Department, Federal University of Juiz de Fora (UFJF) and Smarti9 LTD., Juiz de Fora, Brazil

ARTICLE INFO

Keywords:
Hybrid channel
Power line communication
Wireless communication
Statistical modeling
Channel feature

ABSTRACT

This work aims to increase the understanding and bring the attention to the use of the so-called hybrid power line communication-wireless (PLC-wireless) channel, which is here defined as the equivalent channel that results from the concatenation of PLC and wireless channels, for data communication purposes. In this regard, we discuss about statistical modeling of average channel attenuation, root mean squared delay spread, coherence bandwidth and coherence time, which are among the main features used to characterize data communication channels. Based on a set of measured PLC-wireless channels in in-home facilities, which cover distances lower than 2 m and between 2 m and 6 m, and frequency band between 1.7 MHz and 100 MHz, statistical modeling of the aforementioned set of features is analyzed and compared when several statistical distributions are taken into account. Based on four well-established information criteria, we show the statistical distributions offering the best fits. Furthermore, we show that for the majority of these features, the best two statistical distributions for each of them achieve very similar performance in terms of the chosen information criteria and, as a consequence, both of them may be adopted to statistically model these features.

1. Introduction

Smart grids are the natural evolution of the traditional electric power grids to a new paradigm that embraces intelligence, flexibility, reliability and renewable energy sources [1]. In smart grids, information and energy may flow in a two-way direction among generation and consumers or prosumers [2]. To fulfill these two-way information and energy demands, smart grids heavily rely on telecommunication infrastructures that allow interactions among several entities (e.g., smart meters, smart appliances, smart reclosers and smart transformers) widely spread across the electric power grids.

As detailed in [3], the architectures of telecommunication infrastructures may cover home areas network (HAN), business area network (BAN), neighborhood area network (NAN), metropolitan area network (MAN), rural area network (RAN), centers of operation and substations. Aiming to provide these infrastructures for assisting smart grids deployments, several technologies shall be pursued. Among them, it is interesting to drive the attention to the wired ones, which were designed for coaxial cables, telephone lines, fiber optics and power lines. Regarding wireless solutions, there is a variety of technologies covering licensed and unlicensed frequency bands. The proposition, development and deployment of pervasive or ubiquitous telecommunication infrastructures, which are capable of fulfilling the demands of all players in the smart grids scenario, is still a challenging problem that lacks a definitive solution. This problem is worsened when the concepts of smart city and Internet of Things (IoT) are brought to the center of discussions because the telecommunication infrastructures must be designed to address all of their demands.

Among the aforementioned technologies, the power line communication (PLC) systems have received worldwide attention due to its suitability for fulfilling smart grids demands [4,5]. As a matter of fact, PLC systems constitute an interesting alternative for smart grids due to their pervasive nature, which greatly reduces installation costs and deployment time. Also, PLC can play an important role in smart grids since PLC devices can work as a transceiver and a sensor at the same time [5]. As the majority of electric power system infrastructures are already installed, significant savings on the investment to deploy PLC systems are achieved in comparison to other technologies [6]. Actually,

* Corresponding author.
E-mail addresses: thiago.oliveira@ifsudestemg.edu.br (T.R. Oliveira), picorone@ieee.org (A.A.M. Picorone), camila.zeller@ufjf.edu.br (C.B. Zeller), sergioln@smt.ufrj.br (S.L. Netto), mribeiro@engenharia.ufjf.br (M.V. Ribeiro).

https://doi.org/10.1016/j.epsr.2018.07.004
Received 5 December 2017; Received in revised form 11 June 2018; Accepted 4 July 2018

only wireless technologies are comparable to PLC ones in terms of cost of deployment [4].

Similar to other data communication media, electric power grids show advantages and disadvantages, which are well-reported in the literature. Among them, we bring our attention to the fact the power lines are unshielded and the physical contact with electric power grids for becoming a node in a PLC data network is mandatory. The former fact means that PLC systems can interfere with and suffer from other telecommunication systems operating in the same frequency band. As a result, there are restrictive regulations for using PLC systems around the world (i.e., US, Brazilian and European regulations [7–10]). The latter fact states that we can only access PLC systems with inductive or capacitive coupling devices, which can be a challenging and costly approach when voltage level increases or power lines can not be easily accessed (i.e., underground electric power systems in metropolitan area). Also, the connection of coupling devices to medium- and high-voltage electric power grids demands precaution due the voltage levels [11,12]. In addition, the necessity of physical connection among PLC transceivers and electric power grids cannot allow mobility with PLC systems. As a matter of fact, it has been recognized that mobility can be introduced in PLC systems by assuming that power lines work as antennas [13].

In this context, one may recognize hybrid PLC-wireless channels as an interesting alternative for addressing some emerging telecommunications needs and demands (i.e., smart grids, smart city and IoT). However, proper specification and design of hybrid PLC-wireless data communication systems rely on a complete modeling of these channels through some of their well-established main features. In this direction, some statistical analyses of channel features estimated from a measurement campaign of hybrid PLC-wireless channels in Brazil were presented in [13]. The analyzed channel features comprise average channel attenuation (ACA), root mean squared delay spread (RMS-DS), coherence bandwidth (CB) and coherence time (CT). However, statistical models for hybrid PLC-wireless channels are missing in the literature, something that may postpone or make difficult the dissemination of the usefulness of such kind of channels for assisting the spectrum scarcity problem and the astonishing increase of data communication demands related to smart grids, smart city and IoT.

Aiming to bridge this gap, this paper introduces statistical models for the ACA, RMS-DS, CB and CT features for hybrid PLC-wireless channels. Thus, this work is an important tool to validate future models that can be proposed to represent this kind of communication channel, since mathematical models are usually applied in the design of communication systems. Indeed, several models for some channels features/behaviors can be found in the literature for wireless and PLC channels. In relation to wireless channels, for instance, Rayleigh, Nakagami and Rice statistical models have been used to describe multipath fading envelope, while log-Normal distribution is indicated to model shadowing [14]. In its turn, statistical distributions are used to model some PLC channel features, as can be seen in [15] and [16], where the models are validated through a set of channels measured in Spain and USA, respectively.

In this work the statistical distributions yielding the best models for the considered set of channel features are chosen based on the inspection of the log-likelihood, Akaike information criterion (AIC), Bayesian information criterion (BIC) and the efficient determination criterion (EDC). All statistical modelings address the frequency band ranging from 1.7 MHz up to 100 MHz and take into account two cases for the hybrid PLC-wireless channel: *short-path* channel (up to 2 meters distance far from the outlet) and *long-path* channel (between 2 and 6 meters far from the outlet). The attained results show that the ACA feature is better fitted by the skew-normal distribution for both *short-* and *long-path* channels. Also, the RMS-DS feature is better fitted by the log-logistic distribution for the *short-path* case, whereas the inverse Gaussian is the statistical distribution that best fits the *long-path* case. In addition, the log-normal distribution offers a quite similar RMS-DS fit to the optimal ones in both cases, but it should be avoided for including negative numbers in its support set, whereas the RMS-DS feature is necessarily positive. Regarding the CB feature, the best fit is yielded by the log-logistic distribution for the *short-path* channel, while the t-Student distribution offers the best fit for the *long-path* channel. Finally, the logistic distribution achieves the best fit for CT in the *short-path* channel, whereas the skew-normal distribution provides the best fit for the *long-path* channel.

To introduce these results, the rest of this paper is organized as follows: Section 2 outlines the hybrid PLC-wireless data communication system, while Section 3 summarizes the measurement setup and campaign carried out to measure these channels. Section 4 describes the procedure to estimate the channel parameters considered in this work. Section 5 details the chosen information criteria to evaluate the statistical modeling. Finally, Section 6 focuses on the statistical modeling based on numerical results, while Section 7 emphasizes our concluding remarks.

2. The hybrid PLC-wireless communication system

The use of hybridism within data communication systems is being considered as a promising solution to deal with astonishing and growing demands for telecommunication infrastructures in smart grids, smart city and IoT. The parallel and/or serial deployment of power line communication, wireless communication and visible light communication technologies [17,4] is attractive as it allows one to maximize the usage of channel resources and diversity, thus improving coverage, reliability, flexibility and throughput.

Among all the possible technology combinations, PLC and wireless channels are attracting much attention as the majority of devices/equipments are powered by and connected to an electric power grid and wireless communication has become a pervasive technology. In other words, these devices/equipments can use both the electric power-grid infrastructure and the air for data communication purposes. While the combination of PLC and wireless channels is interesting and, as a consequence, constitute challenging issues for carrying out researches and investigations, there is a very specific combination of PLC and wireless channels that has been forgotten during the past years. In fact, the communication process that starts in a PLC device and ends in a wireless device (or vice versa), through a combination between wireless and PLC channels, was initially considered at the beginning of the past century [18]. Though the lack of tools and technology to push it forward and the focus in wireless-only solutions have reduced or even stopped the development of devices based on this kind of channel. Due to the spectrum scarcity and the increasing demand for data communication, however, all data communication media have to be considered and, as a consequence, the combination of PLC and wireless channels may be re-investigated for assisting the widespread deployment of telecommunication infrastructure in demanding scenarios such as smart grids, smart city and IoT.

In [19], the hybrid PLC-wireless channel, which is defined as the concatenation of PLC and wireless channels, was discussed for data communication purposes. The main idea behind such a channel is to exploit the benefits of electromagnetic unshielded power lines (which is often seen as an undesired characteristic [20,13]), eliminating the necessity of physical connection to these lines. The resulting configuration overcomes the lack of mobility in PLC systems and provides a path through relevant obstacles which often impair the propagation of wireless signals, leading to an alternative, flexible and improved version of PLC systems fulfilling fixed and mobile data communication demands.

Basically, the aim is to provide a hybrid data communication system that is constituted by PLC and wireless transceivers with capacity to communicate with each other in the same frequency band. Such combination can be implemented with the power lines acting as antennas for the PLC transceivers and full-duplex or half-duplex communication

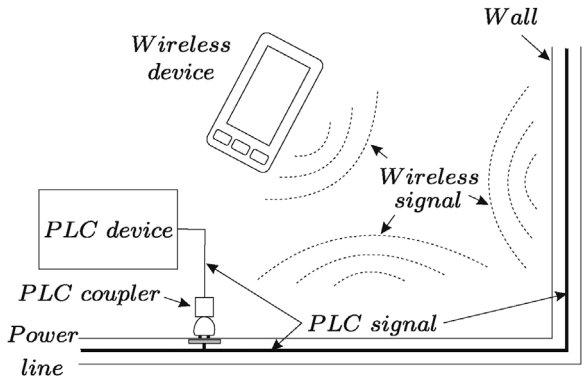

Fig. 1. The hybrid PLC-wireless channel for data communication in indoor scenario.

can be established, as the wireless devices do not need to be physically connected to the power lines, in which PLC signals are being transmitted [21]. Data communication through the hybrid PLC-wireless channel assumes that the PLC transceiver injects signal into or extracts signal from the electric power grids, while the wireless transceiver injects signal into or extracts signal from the air, as depicted in Fig. 1. As both transceivers transmit data in the same frequency band and the signal injected by the PLC transceiver is irradiated in the air and the signal injected in the air by the wireless transceiver is induced into the power lines, then both PLC and wireless transceivers can communicate with each other efficiently [22]. In fact, wireless and PLC transceivers can make use of antennas and PLC coupler devices (inductive or capacitive), respectively, to transmit and to receive signals in the frequency band from 0 MHz to 100 MHz or up to 500 MHz [11].

The following examples can be mentioned to exemplify the advantages associated with the use of this kind of hybrid PLC-wireless channels:

- The electric utilities can access information transfered through the power lines with safety and flexible, regardless the voltage level (high-, medium- or low-voltage) because a contactless approach is considered.
- At the electric utilities side, expressive cost savings can be achieved by reducing the necessity of installation of a PLC-coupler to every access point, as connection is established whenever the wireless device is near the power lines.
- Consumers can monitor and manage their energy consumption usages anywhere and anytime without the necessity of a physical connection to the power line. Also, an interaction with home appliances can be established.
- The range of applications over a hybrid telecommunication infrastructure formed by PLC and wireless devices encompasses network access, sanitation, health care and transportation system, among others.

3. Measurement setup and campaign

The block diagram of the measurement setup for measuring the hybrid PLC-wireless channel is shown in Fig. 2. The transceivers are rugged computers equipped with a high-speed data-acquisition board and a high-speed arbitrary signal-generation board that operate as receiver and transmitter, respectively. Both boards work at a sampling rate of f_s = 200 MHz and all measurements consider the frequency band ranging from 1.7 MHz up to 100 MHz. The antenna is an omnidirectional and monopole one designed to operate in the frequency band ranging from 1 MHz up to 1 GHz and was used to access/submit the signals in the air. The PLC coupler is a capacitive one with almost flat and low attenuation in the frequency band of interest. The coupler was applied to inject/access signals in power line and was assumed as

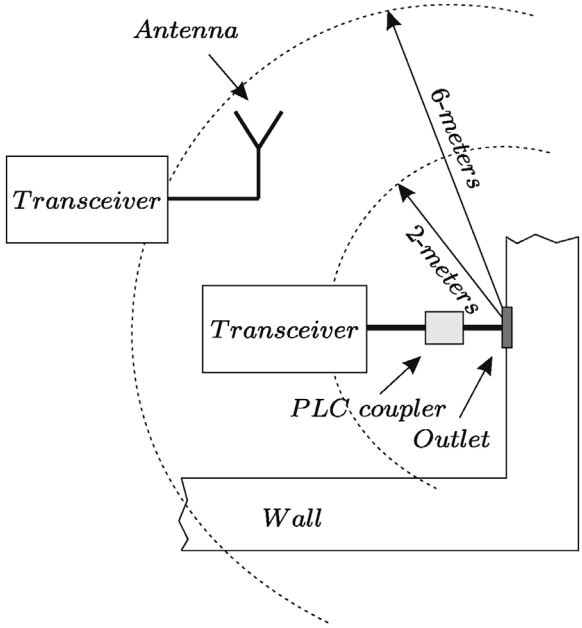

Fig. 2. Measurement setup for the *short-path* (2-m) and *long-path* (6-m) versions of the hybrid PLC-wireless channel.

part of the measured channels.

In order to measure these channels, signal processing techniques that are capable of generating Hermitian symmetric orthogonal frequency division multiplexing (HS-OFDM) signals were used [23,24]. These HS-OFDM signals have $2N$ = 4096 subcarriers, a cyclic prefix of L_{cp} = 512 samples and were injected into the electric power grid through a PLC coupler, which is connected to the PLC transceiver, and extracted from the air with the wireless transceiver, which makes use of an antenna, and vice versa. At the receiver end, a distorted version of the injected signal is measured and stored. With the possession of both transmitted and received HS-OFDM signals, a digital and offline sounding-based approach [25] is performed to estimate the channel frequency response through the following main steps:

(i) The symbol timing synchronization, that is used to estimate the beginning of each received HS-OFDM symbol. This step performs a correlation process and takes advantage of the redundancy presented in transmitted signals due to the presence of the cyclic prefix [26–28].

(ii) The channel frequency response estimation that is preformed in frequency domain, with the transmitted symbol and each received symbol, identified in the previews step. Each channel frequency response estimate has a resolution of Δ_f = 48.83 kHz, approximately. Each channel frequency response estimate is achieved every T_{sym} = 23.04 μs (time duration of each transmitted HS-OFDM symbol). This time interval is much lower than the minimum CT of 600 μs and 1.2 ms observed in-home PLC channels in Spain and Brazil, as pointed out in [29,30], for the frequency band between 1.7 MHz and 30 MHz and between 1.7 MHz and 100 MHz, respectively.

(iii) The channel frequency response estimate enhancement that is applied to reduce the noise interference. This procedure assumes that the channel impulse response effective length (L_h) is lower than the length of the transmitted signal, thus the last samples of the estimated channel impulse response are only due to the noise and are replaced by zero [31]. In this work we have adopted the channel impulse response duration or the number of non-zero coefficients equal to L_{cp} = 512 samples. Thus, an enhanced version of channel frequency response estimates can be given by

Table 1
Main features of the chosen measurement places.

Construction type	Age (years)	Constructed area (m^2)
House # 1	30	78
House # 2	10	69
Apartment # 1	9	54
Apartment # 2	9	42
Apartment # 3	18	65
Apartment # 4	3	62
Apartment # 5	2	54

$\mathbf{H} = \sqrt{2N}\,\mathbf{diag}\{\mathbf{W}\mathbf{h}_{\mathrm{eq}}\}$, where $\mathbf{W}$ is a $2N \times 2N$ matrix that performs the inverse discrete Fourier transform (IDFT), and $\mathbf{h}_{eq} = [h[0], h[1], \ldots, h[L_{cp} - 1], 0, 0, \ldots, 0]^T$ with $(2N - L_{cp})$ zeros. In fact, the adopted methodology renders a channel frequency response from each transmitted symbol, that is, one estimate is achieved every $T_{sym} \approx 23$ μs. On the other hand, by applying a noise reduction by averaging L_{ch} consecutive channel frequency responses, the resulting estimates refer to a time interval corresponding to $L_{ch}T_{sym}$. Thus, the primer procedure seems to be more suitable since the variation over time of measured hybrid PLC-wireless channels is also evaluated in this contribution. In [25], it is shown that the enhancement procedure has almost the same performance in terms of noise reduction than that obtained by averaging eight consecutive channel frequency estimations, in a scenario with additive and white Gaussian noise.

A measurement campaign was held in seven typical places in an urban area of Juiz de Fora, Brazil, as listed in Table 1. During the measurement campaign, potential scattering objects and transceivers were fixed in order to avoid Doppler effects in the wireless portion of the hybrid PLC-wireless channel. Furthermore, by considering the distance between an outlet and a wireless transceiver, see Fig. 2, the following cases were taken into account:

- The *short-path* channel: The wireless transceiver was randomly positioned within a 2-meter distance to the outlet to which the PLC transceiver was connected.
- The *long-path* channel: The wireless transceiver was randomly placed into an area defined as a swept circle, having outer and inner radius of 6 meters and 2 meters, respectively, around the outlet to which the PLC transceiver was connected.

Though the shortest distance between the antenna and the power line cables within the wall seems to be more appropriate than the distance between the antenna and the outlet in which the PLC signal is being injected, the wires location in the wall is not an available information in the measured electrical circuitries. In fact, the measurement campaign was carried out in a random set of residences without any *a priori* knowledge of their electric circuits. We believe that it precisely characterizes the use of PLC systems in residences, which were built without taking into account the data communication through their electric distributions circuits in their specification and design phases.

By taking all facilities into account, 293 different combinations of outlet and wireless transceiver positions were evaluated, in which 201 corresponds to *short-path* channel and 93 refers to the *long-path* channel. For each combination, approximately 600 consecutive estimates (corresponding to 13.8 ms) of the channel frequency response were obtained, rendering a total of 175, 428 channel frequency response estimates of the hybrid PLC-wireless channel.

4. Parameter definitions

The main features of the hybrid PLC-wireless channel considered in this contribution are described as follows.

4.1. Average channel attenuation

The ACA in dB is expressed by

$$\mathrm{ACA} = -10\log_{10}\left(\frac{1}{N}\sum_{k=0}^{N-1}|H[k]|^2\right), \tag{1}$$

where $H[k]$ is the kth coefficient of the discrete channel frequency response related to the zero-padded version of the discrete-time impulse response, obtained through the application of the estimation enhancement procedure described in Section 3.

4.2. Root mean squared delay spread

The RMS-DS represents the distribution of the transmitted power over various paths in a multipath environment, and can be defined as the square root of the second central moment of a power delay profile. For a discrete-time channel impulse response, the RMS-DS (σ_τ) is expressed as

$$\sigma_\tau = T_s\sigma_0 = T_s\sqrt{\mu_0' - \mu_0^2}, \tag{2}$$

where

$$\mu_0 = \frac{\sum_{n=0}^{L_h-1} n\left|h[n]\right|^2}{\sum_{n=0}^{L_h-1}\left|h[n]\right|^2} \quad \text{and} \quad \mu_0' = \frac{\sum_{n=0}^{L_h-1} n^2\left|h[n]\right|^2}{\sum_{n=0}^{L_h-1}\left|h[n]\right|^2}, \tag{3}$$

and $T_s = 1/f_s$ is the sampling period. Note that σ_0 is the RMS-DS normalized to a unitary sampling time, μ_0 is the average delay and $h[n] = h(t)|_{t=\mathrm{n}T_s}$ is the nth sample of the discrete-time channel impulse response. The channel impulse response was considered only in the interval of $n = 0, 1, 2, \ldots, L_{cp} - 1$ for evaluating the RMS-DS feature.

4.3. Coherence bandwidth

The coherence bandwidth reflects how selective the channel frequency response is. Let the correlation function between two frequencies spaced of Δω, given by

$$R(e^{j\omega}) = \int_{-\pi}^{\pi} H(e^{j\omega})H^*(e^{j\omega+\Delta\omega})d\omega, \tag{4}$$

in which $H(e^{j\omega})$ is the Fourier transform of the discrete-time representation of a linear and time invariant PLC channel, $\{h[n]\}_{n=0}^{2N-1}$, and $0 \le \Delta\omega \le 2\pi$. The value of the coherence bandwidth ($\Delta\omega_{B_c}$) in the discrete-time domain is such that

$$|R(e^{j\Delta\omega_{B_c}})| = \gamma|R(1)|, \tag{5}$$

where $0 < \gamma < 1$ is the correlation level informing that the channel frequency response does not vary considerably when $\Delta\omega \in [0, \Delta\omega_{B_c}]$. Assuming a sampling frequency equal to $f_s = 2B$ Hz, in which B is the frequency bandwidth, then the coherence bandwidth (B_c) is expressed as

$$B_c = \frac{\Delta\omega_{B_c}}{2\pi}f_s. \tag{6}$$

The CB estimates from the measured hybrid PLC-wireless channels are analyzed with respect to the correlation coefficient $\gamma = 0.9$, following the majority of previous contributions in the area [32].

4.4. Coherence time

The coherence time is the time duration in which the channel impulse response of a PLC channel is considered time invariant. Following [33], the evaluation of the coherence time may be carried out by assuming that the PLC channel is an wide-sense stationary uncorrelated scattering (WSSUS) process. Then, the coherence time of the channel is

related to the coherence time of the complex gains of the channel, $\alpha_l(t)$, which incorporate both attenuation and phase deviations due to $l = 1, 2, \ldots, L$ multiple reflections of the signal in the communication medium.

In its turn, the coherence index between samples of $\alpha_l(t)$, taken Δt time units apart, is given by

$$\rho_{\alpha_l} = \frac{E[\alpha_l(t)\alpha_l^*(t+\Delta t)]}{E[|\alpha_l^2(t)|]}, \tag{7}$$

in which $E[.]$ is the expectation operator and * denotes the conjugate operator. Thus, it can be assumed that the correlation index of the PLC channel is given by

$$\rho_h(\Delta t) = \frac{\sum_{l=1}^{L} P_l \rho_{\alpha_l}(\Delta t)}{\sum_{l=1}^{L} P_l}; \quad 0 \le |\rho_h(\Delta t)| \le 1, \tag{8}$$

where $P_l = E[|\alpha_l^2(t)|]$ is the average power of the lth path. Hence, the CT of the channel can be obtained through

$$|\rho_h(T_c^\beta)| \ge \beta, \tag{9}$$

where $0 < \beta < 1$ refers to the minimum correlation index admitted to characterize the channel as time-invariant during the time interval $\Delta t = T_c^\beta$. By adopting an hermitian symmetric orthogonal frequency division multiplexing (HS-OFDM) scheme, which is the version of the orthogonal frequency division multiplexing (OFDM) scheme for base-band data communication, the CT for the correlation index β, denoted by T_c^β, can be estimated by using [33]

$$T_c^\beta = M_c(2N + L_{\text{cp}})T_s, \tag{10}$$

where M_c is the number of consecutive channel estimates that is needed to reach a correlation equal to $0 < \beta < 1$, where $T_s = 1/f_s$ denotes the sampling period, $2N$ is the number of subcarriers and L_{cp} is the length of the cyclic prefix in the HS-OFDM symbol.

5. Fit evaluation criteria

The suitability of the set of statistical distributions, which were used to model the data set that represents each considered channel feature (ACA, RMS-DS, CB and CT), were evaluated in terms of the information criteria described below.

5.1. Maximum likelihood estimation

The maximum likelihood estimate (MLE) is referred to as [34]

$$\hat{\theta} = \text{argmax}_\theta \ \rho(\theta), \tag{11}$$

where

$$\rho(\theta) = \sum_{i=1}^{n} \log(f(x_i|\theta_1, \ldots, \theta_K)) \tag{12}$$

is the likelihood function of a random variable with probability density function (pdf) $f(x|\boldsymbol{\theta})$ and $\boldsymbol{\theta} = [\theta_1, \ldots, \theta_K]^T$ is a vector constituted by K unknown elements.

5.2. Information criteria

The Akaike information criterion (AIC), the Bayesian information criterion (BIC) and the efficient determination criterion (EDC) [35] were also applied to increase the confidence in choosing a certain statistical distribution to model the parameters that were obtained from the data set constituted by the estimates of the hybrid PLC-wireless channel.

The three aforementioned information criteria can be calculated by using [35]

$$-2\rho(\hat{\theta}) + \text{Kc}_n, \tag{13}$$

Table 2
Penalty term c_n for AIC, BIC and EDC.

Criterium	c_n
AIC	2
BIC	$\log(n)$
EDC	$0.2\sqrt{n}$

Table 3
Values for the parameter adopted in the estimation process of the analyzed channel features.

Parameter description	Value
Sampling frequency	f_s = 200 MHz
Analyzed frequency band	1.7 MHz up to 100 MHz
Number of sub-carriers in HS-OFDM symbols	$2N$ = 4096
Cyclic prefix length of HS-OFDM symbols	L_{cp} = 512
Channel frequency response resolution	Δ_f = 48.83 kHz
HS-OFDM symbol duration	T_{sym} = 23.04 μs
Correlation coefficient for coherence bandwidth calculus	γ = 0.9
Correlation coefficient for coherence time calculus	β = 0.9

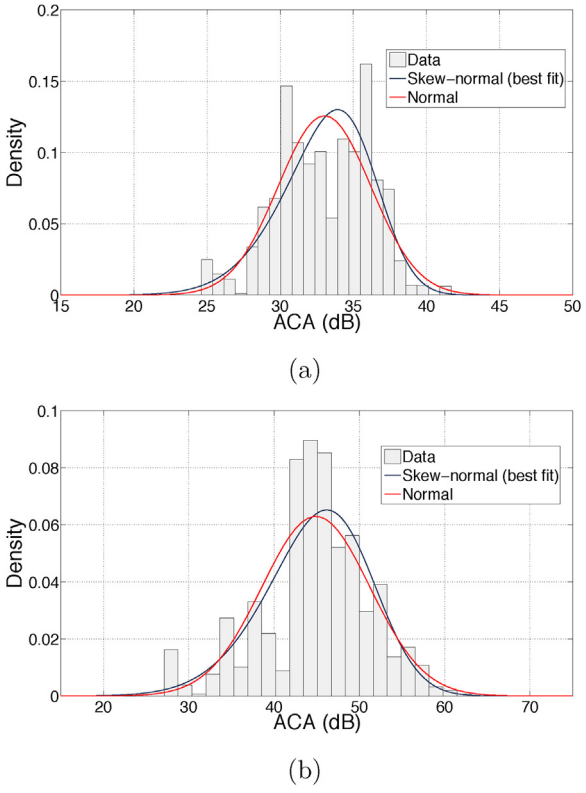

Fig. 3. ACA histograms and best-fitted distributions for: (a) the *short-path* channel and (b) the *long-path* channel.

where K is the number of parameters of the statistical model and c_n is the penalty term, which varies according to Table 2, where n is the data set size. As can be noted in (13), these criteria introduce a term (Kc_n) that penalizes the number of parameters of a given statistical distribution, allowing a fair comparison among the fits attained with statistical distributions with different numbers of parameters. Based on the chosen set of statistical distributions, we have $K = 1, 2, 3$. Different from the log-likelihood function, a lower value for an information criterion (see (13)) indicates a better fit in favor of a given statistical distribution.

Table 4
Results for the best two statistical distributions for modeling ACA (dB).

Distribution	Parameter estimate	Log-likelihood	AIC	BIC	EDC
ACA for the short-path channel					
Skew-normal	$\mu = (33.0600 \pm 0.0016)$ $\sigma = (3.1998 \pm 0.0010)$ $\gamma = (-0.4696 \pm 0.0003)$	-1.6670×10^4	3.3347×10^4	3.3352×10^4	3.3389×10^4
Normal	$\mu = (33.0315 \pm 0.0015)$ $\sigma = (3.1704 \pm 0.0008)$	-1.6723×10^4	3.3449×10^4	3.3453×10^4	3.3478×10^4
ACA for the long-path channel					
Skew-normal	$\mu = (44.8678 \pm 0.0206)$ $\sigma = (6.3050 \pm 0.1137)$ $\gamma = (-0.3703 \pm 0.0019)$	-6.2535×10^3	1.2513×10^4	1.2517×10^4	1.2533×10^4
Normal	$\mu = (44.8971 \pm 0.0208)$ $\sigma = (6.3347 \pm 0.0104)$	-6.2845×10^3	1.2573×10^4	1.2576×10^4	1.2587×10^4

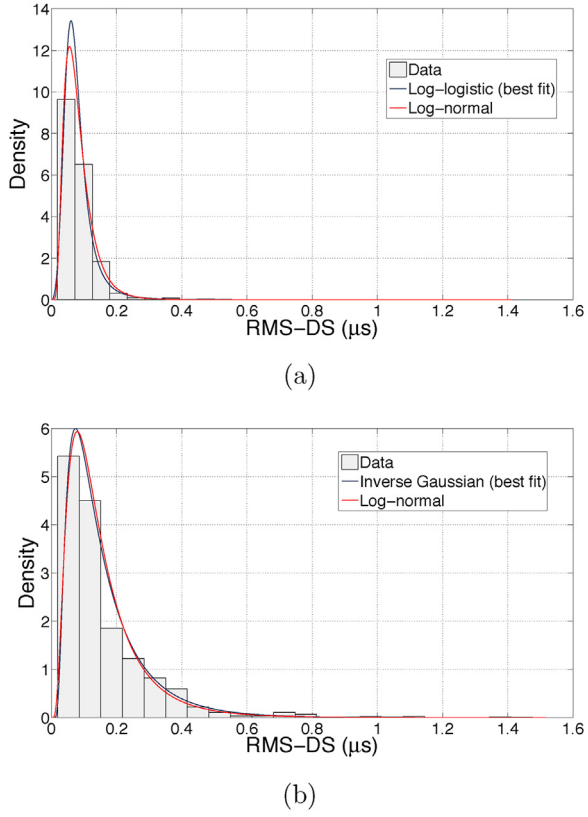

Fig. 4. RMS-DS: (a) the *short-path* channel and (b) the *long-path* channel.

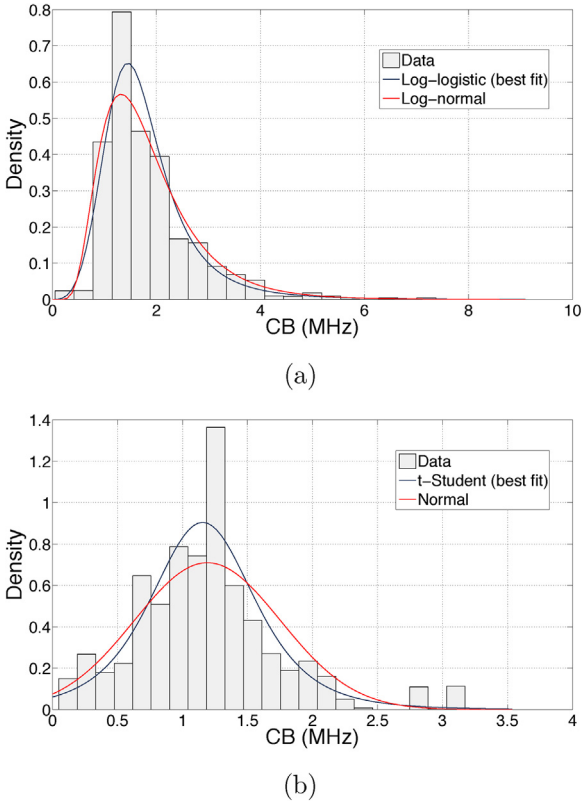

Fig. 5. CB: (a) the *short-path* channel and (b) the *long-path* channel.

6. Results and analysis

This section reports the results of statistical analyses that were carried out in the data sets related to the values of ACA, RMS-DS, CB and CT features. These data sets were obtained from the measured hybrid PLC-wireless channels. Table 3 summarizes the values of several parameters defined in previous sections that are applied in the

Table 5
Results for the best two statistical distributions for modeling RMS-DS (μs).

Distribution	Parameter estimate	Log-likelihood	AIC	BIC	EDC
RMS-DS for the short-path channel					
Log-logistic	$\mu = (-2.6418 \pm 0.3744 \times 10^{-4})$ $\sigma = (0.2835 \pm 0.0854 \times 10^{-4})$	1.2258×10^4	-2.4513×10^4	-2.4509×10^4	-2.4484×10^4
Log-normal	$\mu = (-2.6212 \pm 0.4059 \times 10^{-4})$ $\sigma = (0.5137 \pm 0.2030 \times 10^{-4})$	1.2145×10^4	-2.4287×10^4	-2.4283×10^4	-2.4259×10^4
RMS-DS for the long-path channel					
Inverse Gaussian	$\mu = (0.1620 \pm 0.0786 \times 10^{-4})$ $\sigma = (0.2812 \pm 0.8217 \times 10^{-4})$	2.0492×10^3	-4.0943×10^3	-4.0918×10^3	-4.0808×10^3
Log-normal	$\mu = (-2.0785 \pm 0.2362 \times 10^{-3})$ $\sigma = (0.6743 \pm 0.1182 \times 10^{-3})$	2.0286×10^3	-4.0532×10^3	-4.0506×10^3	-4.0396×10^3

Table 6
Results for the best two statistical distribution for modeling CB (MHz).

Distribution	Parameter estimate	Log-likelihood	AIC	BIC	EDC
CB for the short-path channel					
Log-logistic	$\mu = (0.4961 \pm 0.2835 \times 10^{-4})$	-7.2527×10^{3}	1.4509×10^{4}	1.4513×10^{4}	1.4538×10^{4}
	$\sigma = (0.2482 \pm 0.0660 \times 10^{-4})$				
Log-normal	$\mu = (0.5030 \pm 0.3500 \times 10^{-4})$	-7.6798×10^{3}	1.5364×10^{4}	1.5367×10^{4}	1.5392×10^{4}
	$\sigma = (0.4770 \pm 0.1750 \times 10^{-4})$				
CB for the long-path channel					
	$\mu = (1.1553 \pm 1.2428 \times 10^{-4})$	-1.5371×10^{3}	3.0802×10^{3}	3.0840×10^{3}	3.1005×10^{3}
t-Student	$\sigma = (0.4146 \pm 1.5709 \times 10^{-4})$				
	$\nu = (4.0431 \pm 0.1717)$				
Normal	$\mu = (1.1914 \pm 0.1641 \times 10^{-3})$	-1.6217×10^{3}	3.2473×10^{3}	3.2499×10^{3}	3.2609×10^{3}
	$\sigma = (0.5620 \pm 0.0821 \times 10^{-3})$				

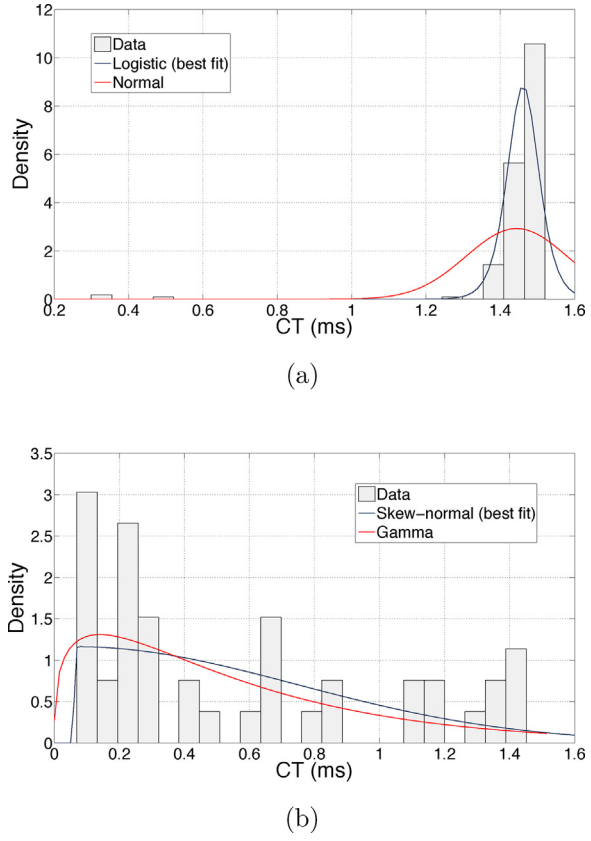

Fig. 6. CT: (a) the *short-path* channel and (b) the *long-path* channel.

estimation process of the channel features considered in this contribution.

As our main purpose is to obtain statistical models for the chosen features, all discussions and results will be based on the histograms associated with the data sets for the ACA, RMS-DS, CB and CT parameters. For the sake of simplicity and convenience, we adopt the density for the amplitude of the histogram as it allows one to visualize the suitability of the best two statistical models for each feature. Also, some variations for the number of bins in the analyzed histograms were tested, but no significant variation was observed in the achieved statistical models. We have decided also to provide the analysis of only the best two statistical distributions in order to facilitate the discussion of statistical modeling, as it may be cumbersome to address all other statistical distributions simultaneously. Furthermore, it is important to emphasize that the information criteria, described in Section 5, are the objective values that allow us to decide in favor of one of the considered statistical distributions.

Since all ACA, RMS-DS, CB and CT values are real random variables, then their statistical models can be properly obtained by considering only some real symmetric and asymmetric statistical distributions. Additionally, it is important to emphasize that some of these features can only assume positive values. Thus careful attention must be driven to choose the best statistical distribution to model the features according to their supports, which can be easily observed by taking a look at the histograms. In this regard, the statistical distributions chosen to be candidate are as follows [36]: (i) symmetric - logistic, normal and *t*-Student; (ii) asymmetric - exponential, Gamma, inverse Gaussian, log-logistic, log-normal, Nakagami, Rayleigh, Rician, skew-normal and Weibull. Note that this set of statistical distributions was chosen because it covers well-established statistical distributions in the data communication field and others in which the support is $\mathbb{R}_+$.

It is important to emphasize that the CB and CT values can be between 0 and ∞; however, the values reported in Table 3, which are considered in this contribution, show that these features are lower bounded by 48.83 kHz and 23.04 μs, respectively.

Table 7
Results for the best two statistical distribution for modeling CT (ms).

Distribution	Parameter estimate	Log-likelihood	AIC	BIC	EDC
CT for the short-path channel					
Logistic	$\mu = (1.4616 \pm 0.9653 \times 10^{-5})$	277.1460	−550.2919	−549.6856	−548.6210
	$\sigma = (0.0282 \pm 0.3190 \times 10^{-5})$				
Normal	$\mu = (1.4439 \pm 0.9218 \times 10^{-4})$	116.1389	−228.2778	−227.6714	−226.6068
	$\sigma = (0.1361 \pm 0.4643 \times 10^{-4})$				
CT for the long-path channel					
	$\mu = (0.6079 \pm 0.0176)$	−14.8528	35.7058	34.5755	33.5942
Skew-normal	$\sigma = (0.4130 \pm 0.0339)$				
	$\gamma = (0.9951 \pm 0.0067)$				
Gamma	$a = (1.3282 \pm 0.0683)$	−17.2225	38.4449	37.6914	37.0372
	$b = (0.4271 \pm 0.0103)$				

6.1. Average channel attenuation

Statistical analyses of ACA, which were calculated from the measured hybrid PLC-wireless channels, show, as it is expected, that the *short-path* channel suffers less attenuations than the *long-path* one, as exemplified in Fig. 3. In fact, while the ACA in *short-path* channels can only reach approximately 42 dB, values as high as 61 dB may be observed in the *long-path* channel. Furthermore, the attained results showed that the ACA is better fitted by the skew-normal distribution in both *short-* (Fig. 3a) and *long-path* (Fig. 3b) channels as stated by all information criteria values listed in Table 4, where SE is the estimated standard fit error. For comparison purposes, both fitted skew-normal and normal distributions are shown in Fig. 3, as both of them achieved the best statistical modeling results.

By taking a look at Fig. 3, the asymmetry of the histograms associated with the ACA in both cases, *short-* and *long-path* channels, is not clear. However, the ACA asymmetry can be inferred by looking at Table 4. As it can be noted, the estimated values for (μ, σ) for the skew-normal and normal distributions are quite close, but the skew-normal distribution achieves the best fit by introducing a negative skewness (asymmetry) through its third parameter (γ).

Regarding the *short-* and *long-path* channels, the obtained parameters for the best fit (skew-normal distribution) and the second best (normal distribution) for ACA are summarized in Table 4.

6.2. Root mean squared delay spread

The histograms obtained from the RMS-DS values (see Fig. 4), as given by the estimated hybrid PLC-wireless channels, show a notorious positive asymmetry. Regarding the RMS-DS values related to the *short-path* channel, one can see that the histograms are better fitted by the log-logistic statistical distribution, while the inverse Gaussian one yields the best fit for the *long-path* channel. For the sake of comparison, the statistical modeling associated with the log-normal distribution is also presented which offered the second best results, quite similar so to speak to the best fits in both cases, as seen in Fig. 4 and given in Table 5. The estimated values of the parameters of the two best fitted statistical distributions in each case are detailed in Table 5.

6.3. Coherence bandwidth

By adopting the correlation coefficient $\gamma = 0.9$ for CB calculus, we can note that the histograms associated with CB values may change, in terms of symmetry, when *short-* and *long-path* channels are compared. For instance, the CB related to *short-path* channels is better fitted by the log-logistic distribution (see Fig. 5a), whereas the best fit for the *long-path* channel is achieved by the t-Student distribution (see Fig. 5b). Additionally, the second best CB fits (log-normal and normal distributions, respectively) for the *short-* and *long-path* channels are displayed in Fig. 5. The attained results for both channels allow us to emphasize the symmetry differences between the histograms related to the two channel types: the histogram for the *short-path* channel shows a positive asymmetry, while the histogram for the *long-path* channel shows strong evidence of symmetry.

Table 6 summarizes the values of the parameters associated with the best statistical distributions, which were used to model the CB values obtained from the *short-* and *long-path* channels, respectively.

6.4. Coherence time

The CT dataset is shorter than those that represent the ACA, RMS-DS and CB, due to the methodology applied to estimate that feature. While the other channel features are estimated from each channel frequency response, the CT is derived from a set of consecutive channel frequency responses. Also, only those combinations that rendered more than 640 consecutive channel frequency response estimates where used. Indeed the CT dataset is composed by 201 estimates for the *short-path* channel and by only 42 estimates for the *long-path* channel.

The histogram associated with the CT values in the *short-path* channel exhibits some kind of symmetry, which is confirmed by the best fit attained by the logistic distribution, as depicted in Fig. 6a. For this channel, the second best fit is achieved by using a normal distribution, which is also shown in Fig. 6a. Regarding the *long-path* channel, we can state that the best two fits are accomplished by using the skew-normal and Gamma distributions, as given in Fig. 6b.

The information criteria values listed in Table 7 show that there is some discrepancy between the two best statistical models, indicating that the normal and Gamma distributions may not be considered to substitute the logistic and skew-normal distributions, respectively. Characterization for the best two statistical distributions for modeling the histograms of the CT values associated with *short-* and *long-path* channels are listed in Table 7.

Though all scattering objects and transceivers were fixed (stationary), the encountered values of coherence time are justified by the time variation of the PLC channel. Indeed, some electrical appliances present a time-variant behavior, regarding the mains signal (of 50 or 60 Hz), resulting in a variation of the PLC channel [29,37]. Thus, all the CT values estimated from the measured hybrid PLC-wireless channels were taken into account in the statistical analysis, that is, no value was considered as outlier.

7. Conclusion

This work focused on the statistical modeling of the key features for the so-called hybrid PLC-wireless channel, which constitutes an appealing and pervasive telecommunication infrastructure for smart grids, smart city, and IoT. In this context, we have addressed estimates of channel frequency responses obtained from a measurement campaign carried out in seven typical residences in urban areas of Brazil. All analyses covered two cases (*short-* and *long-path*) of hybrid PLC-wireless channels, which had been defined according to the relative distance between an outlet and the wireless transceiver.

The attained results have shown that the average channel attenuation is better fitted by the skew-normal distribution for both *short-* and *long-path* channels. Regarding the channel root mean squared delay spread, it was verified that it is better fitted by log-logistic distribution for the *short-path* channel, whereas the inverse Gaussian distribution provided the best fit in the *long-path* channel. Moreover, it was observed that the log-normal distribution resulted in a quite similar modeling performance in comparison to the best root mean squared delay spread fits for both channel types. Considering the coherence bandwidth feature, the best fits were offered by the log-logistic (*short-path*) and t-Student (*long-path*) distributions. Finally, the logistic distribution resulted in the best fit for *short-path* channel coherence time, whereas the skew-normal distribution provided the best fit for the *long-path* channel.

The statistical models provided here yield a better understanding of the hybrid PLC-wireless channel, allowing one to pursuit further investigations related to this flexible and powerful communication medium. Furthermore, these statistical models can support designing data communication systems that are capable of dealing with the challenging and promising hybrid PLC-wireless channel.

Acknowledgements

The authors would like to thank FINEP, FAPEMIG, CNPq, CAPES, INERGE and Smarti9 LTD for their financial supports.

References

[1] C.H. Hauser, D.E. Bakken, A. Bose, A failure to communicate: next generation communication requirements, technologies, and architecture for the electric power grid, IEEE Power Energy Mag. 3 (2) (2005) 47–55, https://doi.org/10.1109/MPAE.

2005.1405870.
[2] F. Rahimi, A. Ipakchi, Demand response as a market resource under the smart grid paradigm, IEEE Trans. Smart Grid 1 (1) (2010) 82–88, https://doi.org/10.1109/TSG.2010.2045906.
[3] Y. Yan, Y. Qian, H. Sharif, D. Tipper, A survey on smart grid communication infrastructures: motivations, requirements and challenges, IEEE Commun. Surv. Tutor. 15 (1) (2013) 5–20, https://doi.org/10.1109/SURV.2012.021312.00034.
[4] L.d.M.B.A. Dib, V. Fernandes, M.d.L. Filomeno, M.V. Ribeiro, Hybrid PLC/wireless communication for smart grids and internet of things applications, IEEE Internet Things J. (2017), https://doi.org/10.1109/JIOT.2017.2764747 (accepted for publication).
[5] S. Galli, A. Scaglione, Z. Wang, For the grid and through the grid: the role of power line communications in the smart grids, Proc. IEEE 99 (6) (2011) 998–1027, https://doi.org/10.1109/JPROC.2011.2109670.
[6] H. Hrasnica, A. Haidine, R. Lehnert, Broadband PowerLine Communications Network Design, John Wiley & Sons, 2004.
[7] Washington, DC, FCC, "Code of Federal Regulations – Title 47: Telecommunication – Chapter I: FCC Part 15 – Radio Frequency Devices" (2002).
[8] ANATEL, Brazilian resolution for PLC. Retrieved June, 2018, http://legislacao.anatel.gov.br/resolucoes/2009/101-resolucao-527 (2009).
[9] Geneva, Switzerland, IEC 61000-3-8, "Electromagnect Compatibility (EMC) – Part 3: Limits – Section 8: Signaling on Low-Voltage Electrical Installations – Emission levels, Frequency bands and Electromagnect Disturbances levels" (2002).
[10] Geneva, Switzerland, CISPR 22, "Information Technology Equipment – Radio Disturbance Characteristics – Limits and Methods of Measurement" (2002).
[11] L.G. da Silva Costa, A.C.M. de Queiroz, B. Adebisi, V.L.R. da Costa, M.V. Ribeiro, Coupling for power line communications: a survey, J. Commun. Inf. Syst. 32 (1) (2017), https://doi.org/10.14209/jcis.2017.2.
[12] G. Artale, A. Cataliotti, V. Cosentino, D.D. Cara, R. Fiorelli, S. Guaiana, G. Tine, A new low cost coupling system for power line communication on medium voltage smart grids, IEEE Trans. Smart Grid (2016), https://doi.org/10.1109/TSG.2016.2630804 (accepted for publication).
[13] T.R. Oliveira, F.J.A. Andrade, A.A.M. Picorone, H.A. Latchman, S.L. Netto, M.V. Ribeiro, Characterization of hybrid communication channel in indoor scenario, J. Commun. Inf. Syst. 31 (1) (2016), https://doi.org/10.14209/jcis.2016.20.
[14] M.K. Simon, M.-S. Alouini, Digital Communication Over Fading Channels, 2nd ed., Wiley, 2004.
[15] F.J. Canete, J.A. Cortes, L. Diez, J.T. Entrambasaguas, A channel model proposal for indoor power line communications, IEEE Commun. Mag. 49 (12) (2011) 166–174, https://doi.org/10.1109/MCOM.2011.6094022.
[16] S. Galli, A novel approach to the statistical modeling of wireline channels, IEEE Trans. Commun. 59 (5) (2011) 1332–1345, https://doi.org/10.1109/TCOMM.2011.031611.090692.
[17] J. Song, W. Ding, F. Yang, H. Yang, B. Yu, H. Zhang, An indoor broadband broadcasting system based on PLC and VLC, IEEE Trans. Broadcast. 61 (2) (2015) 299–308, https://doi.org/10.1109/TBC.2015.2400825.
[18] M. Schwartz, Carrier-wave telephony over power lines: early history [history of communications], IEEE Commun. Mag. 47 (1) (2009) 14–18, https://doi.org/10.1109/MCOM.2009.4752669.
[19] T.R. Oliveira, C.A.G. Marques, M.S. Pereira, S.L. Netto, M.V. Ribeiro, The characterization of hybrid PLC-wireless channels: a preliminary analysis, Proc. IEEE International Symposium on Power Line Communications and Its Applications (2013) 98–102, https://doi.org/10.1109/ISPLC.2013.6525832.
[20] A.S. de Beer, H.C. Ferreira, A.J. Vinck, Contactless power-line communications, Proc. IEEE International Symposium on Power Line Communications and its Applications (2014) 111–115, https://doi.org/10.1109/ISPLC.2014.6812366.
[21] Y. Qian, J. Yan, H. Guan, J. Li, X. Zhou, S. Guo, D.N.K. Jayakody, Design of hybrid wireless and power line sensor networks with dual-interface relay in iot, IEEE Internet Things J. (2017), https://doi.org/10.1109/JIOT.2017.2725451 (accepted for publication).
[22] M. Gebhardt, F. Weinmann, K. Dostert, Physical and regulatory constraints for communication over the power supply grid, IEEE Commun. Mag. 41 (5) (2003) 84–90, https://doi.org/10.1109/MCOM.2003.1200106.
[23] T.R. Oliveira, W.A. Finamore, M.V. Ribeiro, A sounding method based on OFDM modulation for PLC channel measurement, Proc. IEEE International Symposium on Power Line Communications and Its Applications (2013) 185–190, https://doi.org/10.1109/ISPLC.2013.6525847.
[24] M.V. Ribeiro, G.R. Colen, F.V. de Campos, Z. Quan, H.V. Poor, Clustered-orthogonal frequency division multiplexing for power line communication: when is it beneficial? IET Commun. 8 (2014) 2336–2347, https://doi.org/10.1049/iet-com.2014.0056.
[25] T.R. Oliveira, C.A.G. Marques, W.A. Finamore, S.L. Netto, M.V. Ribeiro, A methodology for estimating frequency responses of electric power grids, J. Control Autom. Electr. Syst. 25 (6) (2014) 720–731, https://doi.org/10.1007/s40313-014-0151-5.
[26] J.-J. van de Beek, P.O. Borjesson, M.-L. Boucheret, D. Landstrom, J.M. Arenas, P. Odling, C. Ostberg, M. Wahlqvist, S.K. Wilson, A time and frequency synchronization scheme for multiuser OFDM, IEEE J. Sel. Areas Commun. 17 (11) (1999) 1900–1914, https://doi.org/10.1109/49.806820.
[27] T.-D. Chiueh, P.-Y. Tsai, OFDM Baseband Receiver Design for Wireless Communications, Wiley, 2007.
[28] T. Keller, L. Hanzo, Orthogonal frequency division multiplex synchronization techniques for wireless local area networks, Proc. IEEE International Symposium on Personal, Indoor and Mobile Radio Communications, vol. 3 (1996) 963–967, https://doi.org/10.1109/PIMRC.1996.568424.
[29] F.J.C. Corripio, J.A.C. Arrabal, L.D. del Rio, J.T.E. Munoz, Analysis of the cyclic short-term variation of indoor power line channels, IEEE J. Sel. Areas Commun. 24 (7) (2006) 1327–1338, https://doi.org/10.1109/JSAC.2006.874402.
[30] T.R. Oliveira, A.A. Picorone, S.L. Netto, M.V. Ribeiro, Characterization of Brazilian in-home power line channels for data communication, Electr. Power Syst. Res. 150 (Suppl. C) (2017) 188–197, https://doi.org/10.1016/j.epsr.2017.05.011 http://www.sciencedirect.com/science/article/pii/S0378779617302006.
[31] D. Cardoso, F. Backx, R. Sampaio-Neto, Improved pilot-aided channel estimation in zero padded MC-CDMA systems, 4th International Symposium on Wireless Pervasive Computing (2009) 1–5, https://doi.org/10.1109/ISWPC.2009.4800586.
[32] M. Tlich, A. Zeddam, F. Moulin, F. Gauthier, Indoor power-line communications channel characterization up to 100 MHz – part II: Time-frequency analysis, IEEE Trans. Power Deliv. 23 (3) (2008) 1402–1409, https://doi.org/10.1109/TPWRD.2007.916095.
[33] A.A.M. Picorone, R. Sampaio-Neto, M.V. Ribeiro, Coherence time and sparsity of Brazilian outdoor PLC channels: a preliminary analysis, Proc. IEEE International Symposium on Power Line Communications and Its Applications (2014) 1–5, https://doi.org/10.1109/ISPLC.2014.6812337.
[34] A.M. Mood, F.A. Graybill, D.C. Boes, Introduction to the Theory of Statistics, 3rd ed, McGraw Hill, 1974.
[35] C.R.B. Cabral, V.H. Lachos, C.B. Zeller, Multivariate measurement error models using finite mixtures of skew-student t distributions, J. Multivariate Anal. 124 (C) (2014) 179–198, https://doi.org/10.1016/j.jmva.2013.10.017.
[36] G. Casella, R.L. Berger, Statistical Inference, 2nd ed., Duxbury, 2002.
[37] K. Dostert, Powerline Communications, Prentice-Hall, 2001.